Entrainment range of nonidentical circadian oscillators by a light-dark cycle

Changgui Gu,[1,*] Jinshan Xu,[2] Zonghua Liu,[3] and Jos H. T. Rohling[1,†]
[1]*Department of Molecular Cell Biology, Laboratory for Neurophysiology, Leiden University Medical Center, Leiden, 2300 RC, The Netherlands*
[2]*College of Computer Science, Zhejiang University of Technology, Hangzhou 310023, China*
[3]*Department of Physics, East China Normal University, Shanghai 200062, China*
(Received 28 February 2013; published 2 August 2013)

The suprachiasmatic nucleus (SCN) is a principal circadian clock in mammals, which controls physiological and behavioral daily rhythms. The SCN has two main features: Maintaining a rhythmic cycle of approximately 24 h in the absence of a light-dark cycle (free-running period) and the ability to entrain to external light-dark cycles. Both free-running period and range of entrainment vary from one species to another. To understand this phenomenon, we investigated the diversity of a free-running period by the distribution of coupling strengths in our previous work [Phys. Rev. E **80**, 030904(R) (2009)]. In this paper we numerically found that the dispersion of intrinsic periods among SCN neurons influence the entrainment range of the SCN, but has little influence on the free-running periods under constant darkness. This indicates that the dispersion of coupling strengths determines the diversity in free-running periods, while the dispersion of intrinsic periods determines the diversity in the entrainment range. A theoretical analysis based on two coupled neurons is presented to explain the results of numerical simulations.

DOI: 10.1103/PhysRevE.88.022702 PACS number(s): 87.18.Yt, 05.45.Xt, 87.18.Sn

I. INTRODUCTION

In mammals, a master clock located in the suprachiasmatic nucleus (SCN) controls physiological and behavioral daily rhythms [1–4]. The SCN is composed of tens of thousands of self-sustained oscillating neurons. These individual neurons have nonidentical intrinsic periods ranging from 22 to 28 h, and synchronize to form a unitary SCN output [5,6]. On the one hand, the SCN can sustain a rhythmic output that has a free running period close to but not exactly 24 h under constant darkness. On the other hand, the SCN is capable of adapting its endogenous period to the external light-dark cycle [7–11].

The neurons of SCN form a heterogeneous network, which is often divided into two major subnetworks, a ventrolateral (VL) and a dorsomedial (DM) subnetwork [12–14]. Both subnetworks contribute to the SCN output, but they play different roles in the processing of light input information. The light input originates from the retina and enters the VL via the retinohypothalamic tract. About 25% of the total number of neurons in the SCN are light responsive [14,15]. The VL relays information to the DM, whereas the DM has few feedbacks to the VL. The neurotransmitters in the VL and DM differ [16–19]. The most important neurotransmitter in the VL is a vasoactive intestinal polypeptide (VIP), while the DM neurons are mainly characterized by arganine-vasopressin (AVP). Periods may vary in different regions of the SCN, with the DM running faster than the VL in slice cultures [20]. The VL and DM normally synchronize their periods through coupling pathways containing γ-aminobutyric acid (GABA). With a light-dark cycle that is outside the entrainment range of the SCN, the VL and DM can loose their synchronization. For example, in a 22 h light-dark cycle, in some rats, the VL is entrained to the external 22 h cycle, while the DM keeps its period close to the SCN endogenous period [21,22].

The entrainment range of an animal is defined as the range between its lower limit of entrainment and its higher limit of entrainment [9,10]. Experiments have revealed that the entrainment range differs from one species to another [3]. For example, the entrainment range is from 23.5 h (lower limit of entrainment) to 24.9 h (higher limit of entrainment) for *Peromyscus leucopus*, from 22.8 to 26.5 h for *Mus musculus*, from 21.5 to 28.6 h for *Homo sapiens*, and from 14.9 to 32.4 h for *Eutamias sibiricus* [23]. For simplicity, either the lower limit of entrainment or the higher limit of entrainment is often used to represent the entrainment range, provided that the lower limit of entrainment and the higher limit of entrainment are symmetrically distant from the free-running period. In the present study we used the lower limit of entrainment (LLE) to represent the entrainment range of the SCN.

Two characteristic features of the SCN are the diversity of free-running periods in the absence of an external light-dark cycle among species and differences in the entrainment range. To understand these features, much experimental and theoretical work has been done [4,9,21,24–38]. These studies pointed out that the coupling (mainly through neurotransmitters, e.g., VIP, AVP, and GABA) is a very important characteristic for both features. Coupling not only synchronizes the nonidentical neurons, resulting in one single free-running period, but also plays a role in the ability of the SCN to entrain to a light-dark cycle [29–35]. However, the intrinsic properties of a single neuron have not received much attention. Experiments show that the synchronization of the SCN neurons is influenced by both the coupling properties and the properties of single neurons in aging animals [39]. According to the best of our knowledge, no theoretical work focuses on the effect of nonidentical neuronal oscillators on the overall SCN output. Considering that the intrinsic period among single neurons varies [5,6], we will analyze how the dispersion of periods

*Corresponding author: gu_changgui@163.com
†Corresponding author: J.H.T.Rohling@lumc.nl

influences the entrainment range of the SCN based on a Poincaré model.

The remainder of this paper is organized as follows. In Sec. II we introduce the Poincaré model. In Sec. III we discuss the effect of dispersion of periods among neurons on the free-running behavior of the SCN in absence of a light-dark cycle. In Sec. IV we study the effect of dispersed intrinsic periods on the lower limit of the entrainment of the SCN. In Sec. V a two-neuron model is presented to provide a theoretical analysis for the effect of dispersed periods. Finally, we make a discussion and conclusion in Sec. VI.

II. THE POINCARÉ MODEL OF NONIDENTICAL SCN OSCILLATORS

In the field of circadian rhythms two major types of models are used to represent oscillatory behavior. The Goodwin model describes the oscillator in terms of a genetic feedback loop [29–34], while the Poincaré model uses a more general description for oscillators [11,40]. We selected the Poincaré model for our numerical and theoretical analysis because of its generality and more straightforward way for performing theoretical analysis. We verified that using the Goodwin model does give qualitatively similar results.

In this paper we consider the Poincaré model with N nonidentical neuronal oscillators. The oscillators are coupled through a mean field. Only pN neurons are directly sensitive to the light signal, where p is a ratio of the total number of SCN neurons. We refer to the subnetwork that is composed of pN neurons as VL and the subnetwork composed of the remaining $N - pN$ neurons as DM. Two values of p are considered, i.e., $p = 0.25$ resembling the experimental finding that 25% of the neurons in the SCN are light sensitive, and $p = 1$ to compare this situation to a situation where the SCN would be fully sensitive to light input. We use the normal distribution for the dispersion of intrinsic periods of the nonidentical oscillators. The Poincaré model has two variables, x and y, and can be described as follows:

$$\begin{aligned} \dot{x}_i &= \gamma x_i(A_0 - r_i) - \frac{2y_i\pi}{\tau\sigma_i} + gF + L_i, \\ \dot{y}_i &= \gamma y_i(A_0 - r_i) + \frac{2x_i\pi}{\tau\sigma_i}, \quad i = 1,2,\ldots,N, \\ F &= \frac{1}{N}\sum_{i=1}^{N} x_i, \end{aligned} \tag{1}$$

where i denotes the ith oscillator, γ represents the relaxation parameter, and A_0 and $\tau\sigma_i$ represent the amplitude and intrinsic period of the individual oscillator in the absence of a light-dark cycle. Here τ is a constant and is set to be 24 h, and σ_i is satisfied with a normal distribution with mean value 1 and deviation μ. We use μ to represent the dispersion of intrinsic periods for the different individual oscillators. The oscillators are coupled through the mean-field term gF, where g represents the coupling strength and F is the mean value of variable x_i. r_i is the amplitude of the ith oscillator. L_i represents the light term. r_i and L_i, respectively, are defined as

$$r_i = \sqrt{x_i^2 + y_i^2}, \quad i = 1, 2, \ldots, N, \tag{2}$$

$$L_i = \begin{cases} K_f \sin(\Omega t), & i = 1, 2, \ldots, pN, \\ 0, & i = pN + 1, pN + 2, \ldots, N, \end{cases} \tag{3}$$

where K_f represents the light intensity and Ω is the angular frequency of the light-dark cycle. We consider the effect of parameters μ and K_f on the SCN network in the following sections. The other parameters are set as $\gamma = 0.05, A_0 = 1, g = 0.2, \tau = 24$.

In order to measure the degree of synchronization, we introduce the order parameter R defined as

$$R = \frac{1}{N}\left|\sum_{j=1}^{N}\langle e^{i\theta_j}\rangle_t\right|, \tag{4}$$

where $\langle\cdot\rangle_t$ denotes the average over time and $|\cdot|$ means taking the absolute value. The phase θ is defined as $\theta = \arctan\frac{y}{x}$ in the Poincaré model. The phase difference ϕ of the SCN to the light-dark cycle is defined as $\phi = \langle\frac{1}{N}\sum_{j=1}^{N}\theta_j - \Omega t\rangle_t$. The entrainment range of the SCN network is represented by its lower limit of entrainment (LLE) to light-dark cycles [11]. If the difference of periods between the SCN and the light-dark cycle is less than 0.00001 h, the SCN is considered to be entrained [11].

To numerically calculate the equations, we use the fourth order Runga-Kutta method with time steps of 0.01 h. The initial 10^4 h is neglected to avoid the effect of transients. The number of oscillators is $N = 100$, with initial conditions selected randomly from a uniform distribution in the range (0,1) for each of the individual variables x_i and y_i in the model. We have also calculated the case of $N = 400$ and time steps of 0.001 h, which gave similar results (not shown).

III. FREE-RUNNING PERIOD AND LOWER LIMIT OF ENTRAINMENT OF THE SCN

First, we discuss the influence of the dispersion of intrinsic periods on the free-running period, i.e., the case under constant darkness with $K_f = 0$. In this case, there is no difference between the VL and DM. Our numerical simulations show that the dispersion of intrinsic periods will seriously influence the collective behavior of the neurons. With the increase of the dispersion μ, the synchronization order parameter R decreases [Fig. 1(a)]. The order parameter R has two plateaus, showing different synchronization states with different values of μ. At low values of μ (less than 0.2), R is close to 1, indicating that the neurons are well synchronized. At high values of μ (larger than 0.3), R is approximately 0.3, which is an indication of poorly synchronized neurons. Between these two plateaus, i.e., $0.2 < \mu < 0.3$, there is a transition region. In the following we are interested in the region with well synchronized neurons and thus we restrict ourselves to the region of $\mu < 0.2$. The free-running period T_d is always approximate 26 h, and is independent of μ [Fig. 1(b)]. That is, the nonidentity of neurons does not influence the free-running period. We show an example of five randomly chosen oscillators with dispersion $\mu = 0.1$ [Fig. 1(c)]. The period of the five oscillators is the same, indicating that they are well synchronized in phase, even though they show variations in the amplitude of the oscillations.

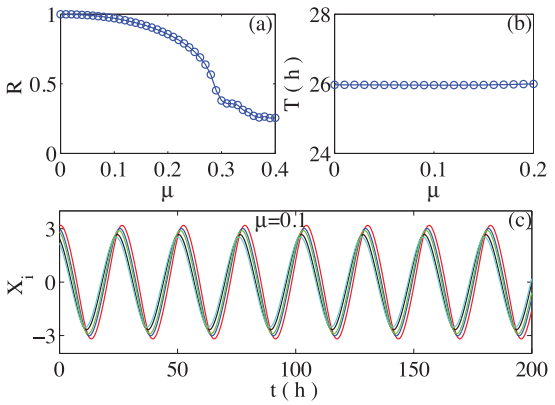

FIG. 1. (Color online) The influence of dispersed intrinsic periods on the behavior of the SCN network in the absence of a light-dark cycle with $N = 100$. (a) The synchronization order parameter R versus dispersion μ. (b) The relationship between the free-running period T_d of the SCN and dispersion μ. (c) Evolution of five randomly chosen oscillators with $\mu = 0.1$.

We continue to study the influence of dispersed intrinsic periods among SCN neurons to the lower limit of entrainment (LLE), where we first consider all neurons to be sensitive to light ($p = 1$). In our previous paper we revealed that a dispersed coupling strength has an effect on the entrainment of the SCN to a light-dark cycle [33]. In this study we find that dispersed intrinsic periods of neurons also influence the ability of the SCN to entrain to external cues. We observe that increasing μ is beneficial for the entrainment range (Fig. 2). In the figure, the y axis is reversed, in order to give the intuition that a lower value of LLE means a broader range of entrainment. For three light intensities K_f, we observe that all curves increase monotonously with μ and their LLE decreased 1 h from dispersion $\mu = 0$ to $\mu = 0.2$, indicating an increase in range of entrainment at $\mu = 0.2$.

To further study LLE, we investigate the properties of the SCN network in terms of the synchronization order parameter R, and the phase difference ϕ of the SCN with regard to the light-dark cycle [Fig. 3(a)]. The order parameter R is close to 1 when μ is near 0, indicating that the neurons are

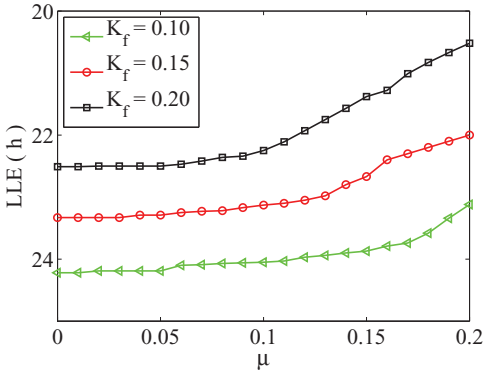

FIG. 2. (Color online) The influence of dispersion μ on the lower limit of the entrainment of the SCN network with $N = 100$ and all neurons are sensitive to light ($p = 1$). Three different light intensities are considered, where the parameter K_f represents the light intensity.

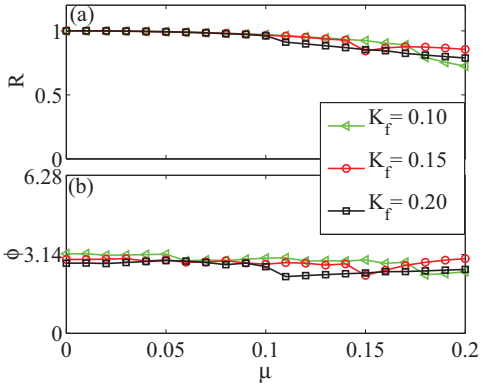

FIG. 3. (Color online) Two properties of the SCN network are considered under the lower limit of entrainment conditions with $N = 100$. (a) Effect of the dispersion μ on the synchronization order parameter R. (b) Effect of the dispersion μ on the phase difference ϕ of the SCN to the light-dark cycle. K_f denotes the light intensity.

perfectly synchronized for each light intensity when the SCN is entrained to the LLE, i.e., the phase difference among neurons is close to 0. When μ is close to 0.2, the order parameter R is about 0.75, which implies that the phase difference among neurons is larger than in the case of μ around 0. The phase difference ϕ between the SCN network and the light-dark cycle when the SCN is entrained at its lower limit of entrainment is around π, and is slightly dependent on the dispersion μ, under each light intensity [Fig. 3(b)]. With $\mu > 0.10$, ϕ is slightly more variable as compared to $\mu \leqslant 0.10$. To get more details about the synchronization (phase difference) among neurons and the phase difference of the SCN to the light-dark cycle, we will check a two-neuron system in the next section.

Finally, we consider the influence on LLE when the SCN is only partially sensitive to light. We take $p = 0.25$ as an example. That is, there are 25% of the SCN neurons sensitive to the external light, and this subset is located in the VL [14]. Similar to the case of full sensitivity to light ($p = 1$, Fig. 2), the range of entrainment increases with increasing μ (Fig. 4). Different values of p and K_f all show comparable results, which suggests that the increase of the range of entrainment with μ is independent of these two parameters.

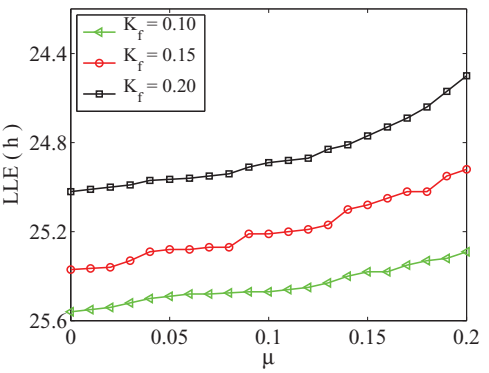

FIG. 4. (Color online) The influence of dispersion μ on the lower limit of entrainment of the SCN network composed of $N = 100$ neurons of which only 25% are sensitive to light. K_f represents light intensity.

An important difference between full and partial sensitivity of the SCN to light is the entrainment range. For full sensitivity to light ($p = 1$) the range of entrainment is broader, indicated by a lower LLE, than when the SCN is only partial sensitive to light ($p = 0.25$). For example, the LLE can reach 20.5 h when the SCN is fully sensitive to light (Fig. 2), while it reaches 24.5 h when it is only partially sensitive to light (Fig. 4), with $K_f = 0.20$ and $\mu = 0.2$. This result can be explained by the fact that the light-sensitive VL part of the SCN can more easily be entrained to shorter external cycles than the light-insensitive DM part [21,22]. This indicates that more light-sensitive neurons would lead a larger range of entrainment, while more light-insensitive neurons would lead to a smaller range of entrainment [33]. In [33], the entrainment ability increases with the value of p.

IV. ANALYSIS OF A SYSTEM WITH TWO COUPLED OSCILLATORS

In this section we will explain the dependence of the LLE on the dispersion μ by analyzing a two-oscillator system. The SCN is physically and functionally divided into two subnetworks, i.e., the VL and DM, where the DM runs faster than the VL [20]. In this section we assume that the VL/DM both act as single oscillators, and the VL oscillates with a lower frequency than the DM.

The system composed of two oscillators is described by the Poincaré model as follows:

$$\begin{aligned}
\dot{x}_a &= \gamma x_a(A_0 - r_a) - \omega_a y_a + g\frac{x_a + x_b}{2} + K_f \sin\Omega t,\\
\dot{y}_a &= \gamma y_a(A_0 - r_a) + \omega_a x_a,\\
\dot{x}_b &= \gamma x_b(A_0 - r_b) - \omega_b y_b + g\frac{x_a + x_b}{2} + K_f \sin\Omega t,\\
\dot{y}_b &= \gamma y_b(A_0 - r_b) + \omega_b x_b,
\end{aligned} \tag{5}$$

where $\omega = \frac{2\pi}{\tau}$, and a and b represent the two oscillators DM and VL, respectively. Without loss of generality, we assume $\omega_a \geqslant \omega_b$. Other parameters are the same as in Eq. (1). For convenience, we transform Eq. (5) from Cartesian coordinates to polar coordinates. Let $x_a = r_a\cos\theta_a$, $y_a = r_a\sin\theta_a$, $x_b = r_b\cos\theta_b$, $y_b = r_b\cos\theta_b$, $\phi_a = \theta_a - \Omega t$, $\phi_b = \theta_b - \Omega t$. Substituting them into Eq. (5) we obtain

$$\begin{aligned}
\dot{r}_a &= \gamma r_a(A_0 - r_a) + \frac{gr_a}{2}\cos^2(\phi_a + \Omega t)\\
&\quad + \frac{gr_b}{2}\cos(\phi_b + \Omega t)\cos(\phi_a + \Omega t)\\
&\quad + K_f \sin\Omega t\cos(\phi_a + \Omega t),\\
\dot{\phi}_a &= \omega_a - \frac{g}{2}\cos(\phi_a + \Omega t)\sin(\phi_a + \Omega t)\\
&\quad - \frac{gr_b}{2r_a}\cos(\phi_b + \Omega t)\sin(\phi_a + \Omega t)\\
&\quad - \frac{K_f}{r_a}\sin\Omega t\sin(\phi_a + \Omega t) - \Omega,\\
\dot{r}_b &= \gamma r_b(A_0 - r_b) + \frac{gr_a}{2}\cos(\phi_a + \Omega t)\cos(\phi_b + \Omega t)\\
&\quad + \frac{gr_b}{2}\cos^2(\phi_b + \Omega t) + K_f \sin\Omega t\cos(\phi_a + \Omega t),\\
\dot{\phi}_a &= \omega_a - \frac{gr_a}{2r_b}\cos(\phi_a + \Omega t)\sin(\phi_b + \Omega t)\\
&\quad - \frac{g}{2}\cos(\phi_b + \Omega t)\sin(\phi_b + \Omega t)\\
&\quad - \frac{K_f}{r_b}\sin\Omega t\sin(\phi_b + \Omega t) - \Omega.
\end{aligned} \tag{6}$$

Considering the averaging method developed by Krylov and Bogoliubov as used in [11,41], ϕ has a lower time scale than Ωt. Letting $\alpha = \langle\phi_a\rangle - \langle\phi_b\rangle$, we get

$$\begin{aligned}
\langle\cos^2(\phi_a + \Omega t)\rangle &= \frac{1}{2},\\
\langle\cos(\phi_b + \Omega t)\cos(\phi_a + \Omega t)\rangle &= \frac{\cos\alpha}{2},\\
\langle\cos(\phi_a + \Omega t)\sin(\phi_a + \Omega t)\rangle &= 0,\\
\langle\cos(\phi_b + \Omega t)\sin(\phi_a + \Omega t)\rangle &= \frac{\sin\alpha}{2},\\
\langle\sin(\Omega t)\cos(\phi_a + \Omega t)\rangle &= \frac{-\langle\sin\phi_a\rangle}{2},\\
\langle\sin(\Omega t)\sin(\phi_b + \Omega t)\rangle &= \frac{\langle\cos\phi_b\rangle}{2},
\end{aligned} \tag{7}$$

where $\langle\cdot\rangle$ denotes the average in one light-dark cycle. Substituting Eq. (7) into Eq. (6) we obtain

$$\begin{aligned}
\langle\dot{r}_a\rangle &= \gamma r_a(A_0 - r_a) + \frac{g}{4}(r_a + r_b\cos\alpha) - \frac{K_f}{2}\langle\sin\phi_a\rangle,\\
\langle\dot{\phi}_a\rangle &= \omega_a - \frac{r_b}{4r_a}g\sin\alpha - \frac{K_f}{2r_a}\langle\cos\phi_a\rangle - \Omega,\\
\langle\dot{r}_b\rangle &= \gamma r_b(A_0 - r_b) + \frac{g}{4}(r_b + r_a\cos\alpha) - \frac{K_f}{2}\langle\sin(\phi_a - \alpha)\rangle,\\
\langle\dot{\phi}_b\rangle &= \omega_b + \frac{r_a}{4r_b}g\sin\alpha - \frac{K_f}{2r_b}\langle\cos(\phi_a - \alpha)\rangle - \Omega.
\end{aligned} \tag{8}$$

For simplicity we keep the nonaveraged notation r_a, r_b, ϕ_a, and ϕ_b in the following. When the SCN is entrained to the light-dark cycle, we have $\dot{r}_a = 0$, $\dot{r}_b = 0$, $\dot{\phi}_a = 0$, and $\dot{\phi}_b = 0$. Equation (8) is simplified as

$$\begin{aligned}
0 &= \gamma r_a(A_0 - r_a) + \frac{g}{4}(r_a + r_b\cos\alpha) - \frac{K_f}{2}\sin\phi_a,\\
\Omega &= \omega_a - \frac{r_b}{4r_a}g\sin\alpha - \frac{K_f}{2r_a}\cos\phi_a,\\
0 &= \gamma r_b(A_0 - r_b) + \frac{g}{4}(r_b + r_a\cos\alpha) - \frac{K_f}{2}\sin(\phi_a - \alpha),\\
\Omega &= \omega_b + \frac{r_a}{4r_b}g\sin\alpha - \frac{K_f}{2r_b}\cos(\phi_a - \alpha).
\end{aligned} \tag{9}$$

In the previous section we have shown that the order parameter $R \approx 1$, i.e., the phase difference among neurons is trivial, and the phase difference ϕ of the SCN to the light-dark cycle is close to π, in the case of $\mu \leqslant 0.1$ (Fig. 3). To obtain more information, we investigated the phase difference of each oscillator to the light-dark cycle, with $N = 2$ and $\mu \leqslant 0.1$ (Fig. 5). The phase difference of both oscillators with respect to the phase of the light-dark cycle is approximately π, which

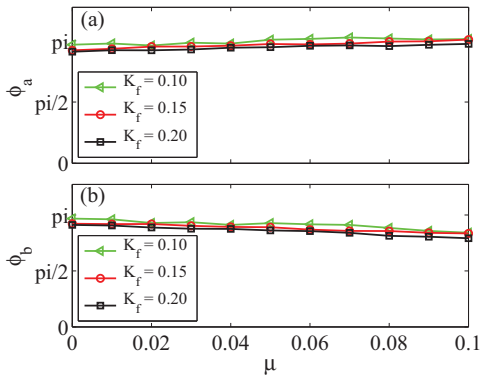

FIG. 5. (Color online) Phase difference of each oscillator to the light-dark cycle versus the dispersion μ with the network size $N = 2$. This figure corresponds to Fig. 3(b). Oscillator a has a larger frequency than oscillator b. (a) The phase difference of oscillator a with respect to the light-dark cycle. The phase difference is little affected by the dispersion μ, and always round π. (b) The phase difference of oscillator b with respect to the light-dark cycle. The phase difference is more affected by the dispersion μ, and declines with increasing dispersion μ. The light intensity is represented by K_f.

implies that the phase difference α between both oscillators is small and the phase difference ϕ of the combined oscillators, representing the SCN, to the light-dark cycle is close to π. This finding is in accordance with the simulation results (Fig. 3). When we consider the phase differences ϕ_a and ϕ_b in more detail, ϕ_a shows little dependence on the dispersion μ and is always close to π, whereas ϕ_b has a negative relationship with the dispersion μ (Fig. 5). In the following part of this section, we assume that the phase difference ϕ_a is a constant π. We desire to give an intuitive explanation for the results shown in Figs. 5 and 3. The value of Ω is related to the intrinsic frequency, the coupling term, and the light term of the second equation in Eq. (7). The maximal contribution of the light term to $\Omega = \Omega_{\rm LLE}$ under the condition $\cos\phi_a \approx -1$, i.e., $\phi_a \approx \pi$. Similarly, for $\Omega = \Omega_{\rm LLE}$ for the fourth equation in Eq. (7), $\phi_b = \phi_a + \alpha \approx \pi$. Furthermore, the phase difference between the oscillators α needs to be small to make $\phi_b \approx \phi_a \approx \pi$. A small value of α is in accordance with the order parameter $R \approx 1$ [Fig. 3(a)].

Let $r_a = r_b + \delta$. α, δ, and K_f are assumed to be small compared to A_0. In the following we approximate α, δ, and K_f to the second order, and take $\phi_a \approx \pi$ [see Fig. 5(a)], under the condition when the SCN is entrained to its LLE. So Eq. (9) can be changed as

$$0 = \gamma r_a(A_0 - r_a) + \frac{g}{4}\left(2r_a - \delta - \frac{r_a\alpha^2}{2}\right), \tag{10}$$

$$\Omega = \Omega_{\rm LLE} = \omega_a - \frac{g\alpha}{4} + \frac{g\alpha\delta}{4r_a} + \frac{K_f}{2r_a}, \tag{11}$$

$$0 = \gamma r_b(A_0 - r_b) + \frac{g}{4}\left(2r_b + \delta - \frac{r_b\alpha^2}{2}\right) - \frac{K_f\alpha}{2}, \tag{12}$$

$$\Omega = \Omega_{\rm LLE} = \omega_b + \frac{g\alpha}{4} + \frac{g\alpha\delta}{4r_a} + \frac{K_f}{2r_b}\sqrt{1-\alpha^2}. \tag{13}$$

Solving Eqs. (10) and (12) we obtain

$$r_a = \frac{\gamma A_0 + \frac{g}{2} - \frac{g\alpha^2}{8} + \sqrt{\left(\gamma A_0 + \frac{g}{2} - \frac{g\alpha^2}{8}\right)^2 - \gamma g\delta}}{2\gamma}$$
$$\approx A_0 + \frac{g}{2\gamma} - \frac{g\alpha^2}{8\gamma} - \frac{g\delta}{4\gamma\left(A_0 + \frac{g}{2\gamma}\right)}, \tag{14}$$

$$r_b \approx A_0 + \frac{g}{2\gamma} - \frac{g\alpha^2}{8\gamma} + \frac{g\delta - 2K_f\alpha}{4\gamma\left(A_0 + \frac{g}{2\gamma}\right)}. \tag{15}$$

Furthermore, $\delta = r_a - r_b = \frac{K_f\alpha - g\delta}{2A_0\gamma + g}$, so we get

$$\delta = \frac{K_f\alpha}{2A_0\gamma + 2g}. \tag{16}$$

Substituting Eq. (16) into Eqs. (14) and (15) we can rewrite r_a and r_a^2 as

$$r_a \approx A_0 + \frac{g}{2\gamma} - \frac{g\alpha^2}{8\gamma} - \frac{gK_f\alpha}{(4\gamma A_0 + 2g)(2A_0\gamma + 2g)},$$
$$r_a^2 \approx \left(A_0 + \frac{g}{2\gamma}\right)^2 - \left(A_0 + \frac{g}{2\gamma}\right)\frac{g\alpha^2}{4\gamma} - \frac{gK_f\alpha}{8\gamma(A_0\gamma + g)}. \tag{17}$$

Letting Eq. (13) − Eq. (11) we get

$$\Delta\omega = \omega_a - \omega_b = -\frac{K_f}{2r_a} + \frac{K\alpha}{2} + \frac{K_f(1-\alpha^2)}{2r_b}$$
$$\approx \frac{K\alpha}{2} - \frac{K_f\alpha^2}{2r_a} + \frac{K_f\delta}{2r_a^2}. \tag{18}$$

From Eq. (18) we obtain

$$2r_a^2\Delta\omega = gr_a^2\alpha - K_f r_a\alpha^2 + K_f\delta. \tag{19}$$

Substituting Eqs. (17) and (16) into Eq. (19) we get

$$0 = 2\Delta\omega\left[\left(A_0 + \frac{g}{2\gamma}\right)^2 - \left(A_0 + \frac{g}{2\gamma}\right)\frac{g\alpha^2}{4\gamma} - \frac{gK_f\alpha}{8\gamma(A_0\gamma + g)}\right] - g\left[\left(A_0 + \frac{g}{2\gamma}\right)^2 - \left(A_0 + \frac{g}{2\gamma}\right)\frac{g\alpha^2}{4\gamma} - \frac{gK_f\alpha}{8\gamma(A_0\gamma + g)}\right]\alpha$$
$$+ K_f\alpha^2\left[A_0 + \frac{g}{2\gamma} - \frac{g\alpha^2}{8\gamma} - \frac{gK_f\alpha}{(4A_0\gamma + 2g)(2A_0\gamma + 2g)}\right] - \frac{K_f^2\alpha}{2A_0\gamma + 2g}. \tag{20}$$

Omitting the terms with the third order and higher for α, for $\Delta\omega$ and for K_f, Eq. (20) becomes

$$0 \approx 2\left(A_0 + \frac{g}{2\gamma}\right)^2\Delta\omega - g\left(A_0 + \frac{g}{2\gamma}\right)^2\alpha. \tag{21}$$

From Eqs. (21), (16), and (14) we get

$$\alpha \approx \frac{2\Delta\omega}{g}, \tag{22}$$

$$\delta \approx \frac{K_f \Delta\omega}{g(A_0\gamma + g)}, \tag{23}$$

$$r_a \approx A_0 + \frac{g}{2\gamma} - \frac{(\Delta\omega)^2}{2g\gamma} - \frac{K_f \Delta\omega}{(4A_0\gamma + 2g)(A_0\gamma + g)}. \tag{24}$$

With Eq. (11) + Eq. (13) we get

$$\Omega_{\mathrm{LLE}} = \frac{\omega_a + \omega_b}{2} + \frac{g\alpha\delta}{4r_a} + \frac{K_f}{4r_a}\left(2 - \frac{\alpha^2}{2}\right) + \frac{K_f\delta}{4r_a^2}. \tag{25}$$

We obtain the analytical result for Eq. (25) after we substitute the parameters α,δ,r_a from Eqs. (22), (23), and (24) into Eq. (25). Furthermore, if we then take the derivative from $\Delta\Omega_{\mathrm{LLE}}$ over $\Delta\omega$ we get

$$\begin{aligned}\frac{d\Omega_{\mathrm{LLE}}}{d\Delta\omega} = {} & \frac{K_f\Delta\Omega}{(A_0\gamma + g)gr_a} \\ & + \frac{g\alpha\delta}{4r_a^2}\left[\frac{\Delta\omega}{g\gamma} + \frac{K_f}{(4A_0\gamma + 2g)(A_0\gamma + g)}\right] \\ & + \frac{K_f}{2r_a^2}\left[\frac{\Delta\omega}{g\gamma} + \frac{K_f}{(4A_0\gamma + 2g)(A_0\gamma + g)}\right] \\ & - \frac{K_f\alpha^2}{8r_a^2}\left[\frac{\Delta\omega}{g\gamma} + \frac{K_f}{(4A_0\gamma + 2g)(A_0\gamma + g)}\right] \\ & - \frac{K_f\Delta\omega}{g^2 r_a} + \frac{K_f^2}{4gr_a^2(A_0\gamma + g)} \\ & + \frac{K_f\delta}{8r_a^3}\left[\frac{\Delta\omega}{g\gamma} + \frac{K_f}{(4A_0\gamma + 2g)(A_0\gamma + g)}\right].\end{aligned} \tag{26}$$

When $\Delta\omega \to 0$, from Eq. (26) we obtain

$$\begin{aligned}\left.\frac{d\Omega_{\mathrm{LLE}}}{d\Delta\omega}\right|_{\Delta\omega\to 0} = {} & \frac{K_f^2}{2r_a^2(4A_0\gamma + 2g)(A_0\gamma + g)} \\ & + \frac{K_f^2}{4gr_a^2(A_0\gamma + g)} > 0.\end{aligned} \tag{27}$$

The dispersion μ in the two-oscillator system is defined as $\mu = |\frac{\tau_a - \tau_b}{\tau_a + \tau_b}| = \frac{\Delta\omega}{\omega_a + \omega_b}$. From Eq. (27) we get $\frac{\mathrm{d}\Omega_{\mathrm{LLE}}}{\mathrm{d}\mu}|_{\mu\to 0} > 0$. Therefore, we have proven that there is a positive relationship between Ω_{LLE} and the dispersion μ of intrinsic periods of SCN neurons, provided that μ is small.

V. DISCUSSION AND CONCLUSION

The main circadian clock, situated in the SCN, shows free-running cycles of about 24 h under constant darkness, and can also be entrained to external light-dark cycles that do not differ too much from 24 h. The free-running period and range of entrainment vary among species. Our previous work [31] gave an alternative explanation for the diversity of free-running periods and proposed that the diversity of the free-running period is caused by the dispersion of coupling strength. So far, no theoretical work has been performed to explain the diversity in entrainment range between species. In this paper we studied the range of entrainment based on dispersed intrinsic periods of neurons using the Poincaré model. Both our numerical simulations and analytical results showed that there is a positive relationship between the range of entrainment and the dispersion of intrinsic periods of SCN neurons. This could provide an alternative explanation for the diversity of entrainment ranges, i.e., species where the intrinsic periods of the SCN neurons are more dispersed have a broader range of entrainment. We have also investigated the effect of dispersion of intrinsic periods on the free-running period, and found that the influence is very small. In conclusion, our work suggest that the entrainment range is influenced by the dispersion of periods among SCN neurons. By the use of the Poincaré model this analysis is not limited to the field of circadian rhythms, but also applies to other systems, such as the synchronous flashing of fireflies.

ACKNOWLEDGMENTS

This work is partially supported by Complexity Grant of the NWO of the Netherlands, No. 645.000.010 and the NNSF of China under Grants No. 11135001 and No. 10975053.

[1] C. S. Pittendrigh and S. Daan, J. Comp. Physiol. A **106**, 333 (1976).
[2] C. S. Pittendrigh, Annu. Rev. Physiol. A **55**, 17 (1993).
[3] M. J. Vansteensel, S. Michel, and J. H. Meijer, Brain Res. Rev. **58**, 18 (2008).
[4] D. K. Welsh, J. S. Takahashi, and S. A. Kay, Annu. Rev. Physiol. **72**, 551 (2010).
[5] D. K. Welsh, D. E. Logothetis, M. Meister, and S. M. Reppert, Neuron **14**, 697 (1995).
[6] S. Honma, W. Nakamura, T. Shirakawa, and K. Honma, Neurosci. Lett. **358**, 173 (2004).
[7] C. A. Czeisler *et al.*, Science **284**, 2177 (1999).
[8] H. Daido, Phys. Rev. Lett. **87**, 048101 (2001).
[9] S. Usui, Y. Takahashi, and T. Okazaki, Am. J. Physiol. Regul. Integr. Comp. Physiol. **278**, R1148 (2000).
[10] A. Campuzano, J. Vilaplana, T. Cambras, and A. Diez-Noguera, Physiol. Behav. **63**, 171 (1998).
[11] U. Abraham, A. E. Granada, P. O. Westermark, M. Heine, A. Kramer *et al.*, Mol. Syst. Biol. **6**, 438 (2010).
[12] J. H. Meijer and W. J. Schwartz, J. Biol. Rhythms **18**, 235 (2003).
[13] H. T. vanderLeest, J. H. Rohling, S. Michel, and J. H. Meijer, PLoS ONE **4**, e4976 (2009).
[14] J. H. Rohling, H. T. vanderLeest, S. Michel, M. J. Vansteensel, and J. H. Meijer, PLoS ONE **6**, e25437 (2011).
[15] J. H. Meijer, G. A. Groos, and B. Rusak, Brain Res. **382**, 109 (1986).
[16] S. J. Aton, C. S. Colwell, A. J. Harmar, J. Waschek, and E. D. Herzog, Nat. Neurosci. **8**, 476 (2005).
[17] H. Albus, M. J. Vansteensel, S. Michel, G. D. Block, and J. H. Meijer, Curr. Biol. **15**, 886 (2005).
[18] R. Silver and W. J. Schwartz, Methods Enzymol. **393**, 451 (2005).
[19] L. P. Morin, J. Biol. Rhythms **22**, 3 (2007).

[20] T. Noguchi, K. Watanabe, A. Ogura, and S. Yamaoka, Eur. J. Neurosci. **20**, 3199 (2004).
[21] H. O. de la Iglesia, T. Cambras, W. J. Schwartz, and A. Diez-Noguera, Curr. Biol. **14**, 796 (2004).
[22] M. D. Schwartz, C. Wotus, T. Liu, W. O. Friesen, J. Borjigin *et al.*, Proc. Natl. Acad. Sci. USA **106**, 17540 (2009).
[23] R. Refinetti, *Circadian Physiology*, 2nd ed. (CRC, Boca Raton, FL, 2006).
[24] H. O. de la Iglesia, J. Meyer, A. Carpino Jr., and W. J. Schwartz, Science **290**, 799 (2000).
[25] S. Yamaguchi, H. Isejima, T. Matsuo, R. Okura, K. Yagita *et al.*, Science **302**, 1408 (2003).
[26] M. Nagano, A. Adachi, K. Nakahama, T. Nakamura, M. Tamada, E. Meyer-Bernstein, A. Sehgal, and Y. Shigeyoshi, J. Neurosci. **23**, 6141 (2003).
[27] H. Ohta, S. Yamazaki, and D. G. McMahon, Nat. Neurosci. **8**, 267 (2005).
[28] L. Yan, N. C. Foley, J. M. Bobula, L. J. Kriegsfeld, and R. Silver, J. Neurosci. **25**, 9017 (2005).
[29] D. Gonze, S. Bernard, C. Waltermann, A. Kramer, and H. Herzel, Biophys. J. **89**, 120 (2005).
[30] J. C. W. Locke, P. O. Westermark, A. Kramer, and H. Herzel, BMC Syst. Biol. **2**, 22 (2008).
[31] C. Gu, J. Wang, and Z. Liu, Phys. Rev. E **80**, 030904(R) (2009).
[32] C. Gu, J. Wang, J. Wang, and Z. Liu, Phys. Rev. E **83**, 046224 (2011).
[33] C. Gu, Z. Liu, W. J. Schwartz, and P. Indic, PLoS ONE **7**, e36900 (2012).
[34] J. Xu, C. Gu, A. Pumir, N. Garnier, and Z. Liu, Phys. Rev. E **86**, 041903 (2012).
[35] S. Bernard, D. Gonze, B. Cajavec, H. Herzel, and A. Kramer, PLoS Comput. Biol. **3**, e68 (2007).
[36] P. Indic, W. J. Schwartz, and D. Paydarfar, J. R. Soc. Interface **5**, 873 (2008).
[37] M. Hafner, H. Koeppl, and D. Gonze, PLoS Comput. Biol. **8**, e1002419 (2012).
[38] C. Bodenstein, M. Gosak, S. Schuster, M. Marhl, and M. Perc, PLoS Comput. Biol. **8**, e1002697 (2012).
[39] S. Farajnia *et al.*, J. Neurosci. **32**, 5891 (2012).
[40] L. Glass and M. C. Mackey, *From Clocks to Chaos: The Rhythms of Life* (Princeton University Press, Princeton, New Jersey, 1998).
[41] A. Balanov, N. Janson, D. Postnov, and O. Sosnovtseva, *Synchronization: From Simple to Complex* (Springer, New York, 2009).